NASA TECHNICAL NOTE

NASA TN D-4786

NASA TN D-4786

LOAD RELIEF AUTOPILOT ANALYSIS TO MINIMIZE LAUNCH VEHICLE PEAK THRUST VECTOR DEFLECTION REQUIREMENTS

by Leslie L. Scalzott and Fred Teren

Lewis Research Center
Cleveland, Ohio

NATIONAL AERONAUTICS AND SPACE ADMINISTRATION • WASHINGTON, D. C. • SEPTEMBER 1968

NASA TN D-4786

LOAD RELIEF AUTOPILOT ANALYSIS TO MINIMIZE LAUNCH VEHICLE PEAK THRUST VECTOR DEFLECTION REQUIREMENTS

By Leslie L. Scalzott and Fred Teren

Lewis Research Center
Cleveland, Ohio

NATIONAL AERONAUTICS AND SPACE ADMINISTRATION

For sale by the Clearinghouse for Federal Scientific and Technical Information
Springfield, Virginia 22151 – CFSTI price $3.00

ABSTRACT

A load relief autopilot design to minimize the maximum thrust vector deflection angle required to maintain vehicle stability during flight through design winds is analyzed. The feedback variables are angle of attack and flight path angle as well as attitude error and rate. A rigid body configuration is assumed, and sensor dynamics are not considered. Deflection angle and attitude error responses are presented for design winds. It is shown that the load relief autopilot analyzed results in a 50 percent decrease in deflection requirements for these winds as compared to a conventional autopilot designed to trim the vehicle.

LOAD RELIEF AUTOPILOT ANALYSIS TO MINIMIZE LAUNCH VEHICLE PEAK THRUST VECTOR DEFLECTION REQUIREMENTS

by Leslie L. Scalzott and Fred Teren

Lewis Research Center

SUMMARY

A load relief autopilot designed to minimize the maximum thrust vector deflection angle required to maintain vehicle stability during flight through design winds is analyzed. The feedback variables are angle of attack and flight path angle as well as attitude error and rate. This autopilot is investigated for a vehicle consisting of a 260-inch solid motor first stage, SIVB second stage, and extended Voyager payload. A rigid body configuration is assumed, and sensor dynamics are not considered.

Deflection angle and attitude error responses are presented for expected flight winds. It is shown that the load relief autopilot analyzed results in a 50 percent decrease in deflection requirements for these flight winds as compared to a conventional autopilot designed to trim the vehicle. It is also demonstrated that the results should apply to most other vehicles, as well as the one simulated.

INTRODUCTION

Due to the limited gimbaling capability of solid fuel rocket vehicles, it is extremely desirable to minimize the maximum thrust vector deflection angle required to maintain vehicle stability while flying through design winds. Stability is defined here as the ability to follow a desired flight path or return to this path after a deviation due to some disturbance. Deflection angle requirements can be reduced by the addition of aerodynamic surfaces (fins or canards; see ref. 1) or by autopilot design. Conventional autopilots are designed to maintain trimmed flight conditions (i.e., to maintain the nominal flight path during the disturbance). Usually, the deflection angle is not permitted to reach its maximum value.

Borsody and Teren (ref. 2) define an ideal autopilot which allows the deflection angle to increase to its maximum value and remain at this value for some finite time. They

further determined the vehicle stability limit; that is, the minimum value of the maximum deflection angle for which the vehicle is stable as defined above. It was demonstrated that with a feasible open loop control, the deflection angle requirement for design winds could be reduced to 56 percent of the trim requirement.

A type of load relief autopilot designed to exploit this advantage is investigated in this report. The feedback variables include angle of attack and flight path angle in addition to the conventional feedback variables of attitude and attitude rate. The approach taken is that a maximum allowable magnitude for the deflection angle δ_{max} is assumed. The minimum value of δ_{max} required for stability is established by reducing δ_{max} until the vehicle becomes unstable for some expected flight wind. The vehicle uses the commanded deflection angle whenever this value is less than δ_{max}. If the commanded deflection angle exceeds the limit, δ_{max} is used. If the system is stable, the commanded deflection angle will return to a magnitude less than δ_{max} after a short time.

The analysis is performed by linearizing about the vehicle equations of motion at constant time. This procedure results in a set of third order equations. The autopilot gain constants are calculated, and the system transfer functions are established. These equations can be reduced to second order by assuming that the winds produce negligible drift in the flight profile. The analysis demonstrates that essentially the same transfer functions result when the vehicle motion is approximated by the second order equations. Therefore, for simplicity, the second order equations are used to obtain most of the results. Later, an integral gain is added to the autopilot in order to guarantee that the vehicle will follow the desired pitch program, even if the autopilot and vehicle parameters are not accurately known. It is found that integral gain does not substantially reduce the effectiveness of the autopilot.

The three sets of vehicle and autopilot equations (third order, second order, and second order with integral gain) are simulated along with triangular wind profiles of varying shape and duration. Results are presented for a typical solid propellant launch vehicle consisting of a 260 inch solid motor first stage, the SIVB second stage and the extended Voyager payload (ref. 3). Maximum deflection angle requirements are presented as a function of wind duration. Typical deflection and vehicle attitude profiles are also presented with and without limited thrust vector deflection angle capability. The equations and results obtained are generalized to apply to other launch vehicles.

ANALYSIS AND ASSUMPTIONS

In order to simplify the analysis and allow a closed form solution, the vehicle equations of motion are linearized about the nominal trajectory at constant time. A rigid body configuration is also assumed. Therefore, vehicle bending, sloshing, and aeroelastic

effects are not considered. The angle of attack sensor and the engine gimbal actuator are assumed to have no appreciable dynamics. The results presented later show that actuator response requirements for the autopilot studied herein are not significantly greater than required for a conventional autopilot designed to trim the vehicle. The flight path angle can be calculated in the guidance computer from the vehicle position and velocity components, which are obtained by integrating the vehicle equations of motion. The dynamics of this loop are also neglected in this report.

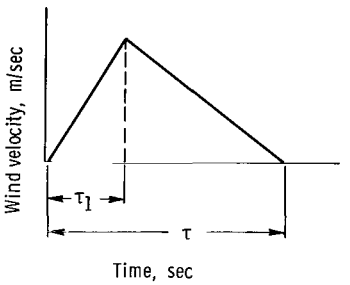

The results are obtained for triangular wind disturbances, with total wind duration τ (see above sketch) ranging from 3 to 20 seconds. Symmetrical triangular wind shapes are investigated extensively, but unsymmetrical shapes are also considered. For the unsymmetrical wind shapes, the disturbance buildup time is varied from 3 to 10 seconds. The variables used are defined in the symbol list (appendix A). A variety of real wind profiles can be approximated by varying the peak wind velocity, duration, and shape of the triangular profile. Also, the synthetic wind profiles developed in a work entitled "Terrestrial Environment (Climatic) Criteria Guidlines for Use in Space Vehicles Development, 1964 Revision" by Glenn E. Daniels of the NASA Marshall Space Flight Center, can be approximated by this method.

The reduction in thrust vector deflection (TVD) requirements obtained herein applies to wind disturbances only. Other TVD requirements, such as TVD required for thrust misalinement, center of gravity offset, pitch program, and vehicle dispersions, are not affected by the autopilot design chosen. However, these requirements are generally much smaller than the TVD required for winds. Therefore, the overall reduction in TVD requirements which will be demonstrated is still very significant.

The autopilot design criteria are as follows:

(1) The control system undamped natural frequency and damping ratio are specified. The damping ratio is set at 0.707, which results in minimum overshoot and rapid settling.

(2) The vehicle attitude should follow the nominal pitch program in the absence of disturbances. That is, $\theta/\theta_p = 1$ at zero frequency.

(3) The maximum deflection angle required to maintain stability when disturbances (winds) are present is to be minimized.

The basic vehicle configuration is presented in figure 1. Many of the variables used in this report are defined in this figure. As shown in figure 1, the vehicle has aerodynamic forces acting on it. These forces may be assumed to be concentrated at a single point, the vehicle center of pressure. Generally, the center of pressure is located above the center of gravity, which results in an aerodynamically unstable vehicle. The vehicle is stabilized by the control system.

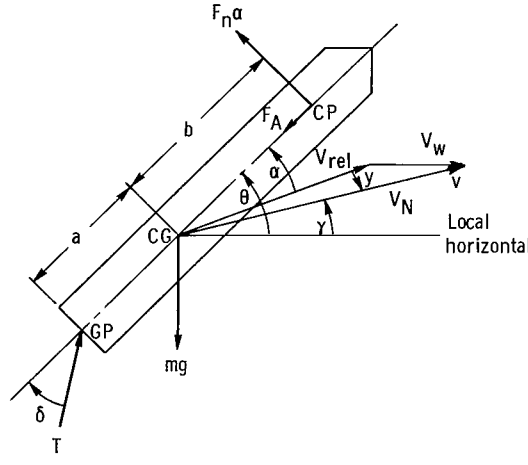

Figure 1. - Basic vehicle configuration.

The derivation of the vehicle and control equations for the second order, third order, and second order plus integral gain systems is presented in appendix B. The equations are derived in a cartesian coordinate system whose axes are oriented along and perpendicular to the vehicle flight path. The origin of the coordinate system is located at the center of gravity of the vehicle. Although the equations are derived for the pitch plane, they are easily modified for the yaw plane, as shown in the equation derivations.

The linearized equations of motion in the pitch plane (eq. (B1)) are:

$$\Delta\ddot{\theta} = \mu_c\delta + \mu_\alpha\alpha$$

$$\alpha = \Delta\theta - \Delta\gamma + y$$

$$\Delta\dot{\gamma} = \frac{1}{mv_N}\left[(T - F_A)\,\Delta\theta - (T - F_A - mg\sin\gamma_N)\,\Delta\gamma - T\delta + F_n\alpha\right]$$

$$\Delta\dot{v} = - g \cos \gamma_N \Delta\gamma$$

$$y = \frac{v_w}{v_N} \sin \gamma_N$$

where y is the wind angle resulting from the wind disturbance, as illustrated in figure 1. The wind angle may be calculated from the wind velocity, nominal flight path angle, and vehicle relative velocity, as shown in equation (B1c). Also, since a fixed time analysis is used, the wind duration may be related to altitude interval by multiplying by the vehicle vertical velocity:

$$\text{Altitude interval of wind} = \tau v_N \sin \gamma_N$$

The nominal flight is assumed to be zero angle of attack with no wind. The control equation is:

$$\delta = K_p \theta_p - K_\theta \Delta\theta - K_R \Delta\dot{\theta} - K_\gamma \Delta\gamma - K_\alpha \alpha$$

The desired pitch program is satisfied by proper choice of the gain constants as a function of K_α. The derivation is presented in appendix B, but the major results are repeated here. The required values of the gain constants are:

$$K_p = \frac{\omega_n^2}{\mu_c}$$

$$K_\theta = \frac{\omega_n^2 + \mu_\alpha}{\mu_c} - K_\alpha$$

$$K_R = \frac{2\zeta\omega_n}{\mu_c}$$

$$K_\gamma = K_\alpha - \frac{\mu_\alpha}{\mu_c}$$

With these gain constants, the vehicle attitude and control responses become:

$$\frac{\Delta\theta}{\theta_p} = \frac{\mu_c K_p}{\left(s^2 + 2\zeta\omega_n s + \omega_n^2\right)}$$

$$\frac{\Delta\theta}{y} = \frac{(\mu_\alpha - \mu_c K_\alpha)}{\left(s^2 + 2\zeta\omega_n s + \omega_n^2\right)}$$

$$\frac{\delta}{\theta_p} \approx \frac{K_p\left(s^2 - \mu_\alpha\right)\left(s - \dfrac{g \sin \gamma_N}{v_N}\right)}{\left(s^2 + 2\zeta\omega_n s + \omega_n^2\right)(s + c)}$$

$$\frac{\delta}{y} \approx \frac{-\left(K_\alpha s^2 + \mu_\alpha K_R s + \mu_\alpha K_\theta\right)\left\{s + \dfrac{\dfrac{1}{mv_N}\left[(T - F_A - mg \sin \gamma_N)K_\theta + (T - F_A)K_\gamma\right]}{K_\theta}\right\}}{\left(s^2 + 2\zeta\omega_n s + \omega_n^2\right)(s + c)}$$

where

$$c = \frac{\left(1 + \dfrac{\mu_\alpha}{\mu_c}\right) T + F_n - F_A - mg \sin \gamma_N}{mv_N}$$

The pole location c is set equal to the zero of $\Delta\theta/\theta_p$. This reduces the $\Delta\theta/\theta_p$ response to second order, which will be discussed later. The pitch program response $\Delta\theta/\theta_p$ is specified by adjusting K_p so that the control system follows the pitch program in the absence of disturbances. Also, the value of K_α can be chosen to minimize the deflection angle necessary to maintain stability when disturbances are present.

A second order approximation to the equations of motion is also investigated. This simplification is desirable since it permits a better understanding of the system. By comparing the second and third order equations, the effect of the additional zero and pole can be determined. Also, the effect of an integral gain term added to the system can be more easily observed by comparison with a second order system. The second order approximation is derived by assuming that the flight path angle does not deviate from the nominal ($\Delta\gamma = 0$). For this case, the control equation is:

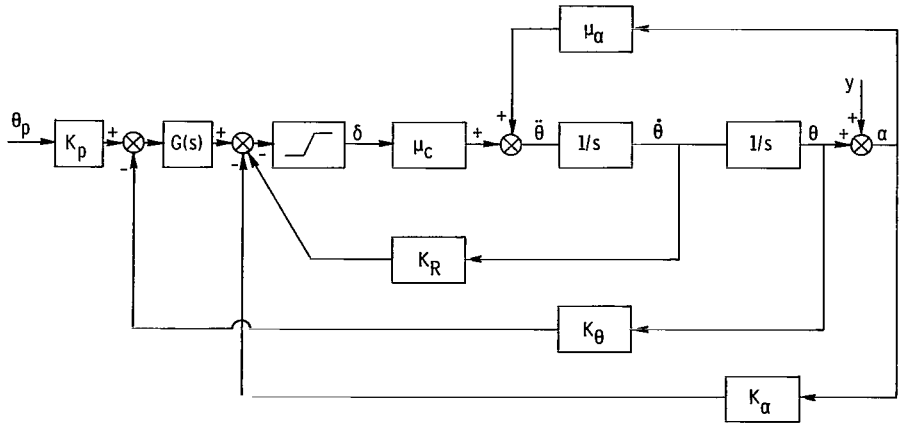

Figure 2. - Second-order block diagram. Without integral gain: G(s) = 1. With integral gain: $K_\theta = K_p$; $G(s) = (1 + K_I/s)$.

$$\delta = K_p\theta_p - K_\theta \Delta\theta - K_R \Delta\dot{\theta} - K_\alpha\alpha$$

A block diagram of the second order system is presented in figure 2. Appendix B presents the second, as well as the third order equations and the response solutions. Comparison of these response equations demonstrates that the second order equations very closely approximate the third order system under investigation. It is shown that the large-valued poles and zeroes are identical for the two systems, leaving a small pole and zero in the deflection angle response equations. These roots are small and do not contribute appreciably to the response transients.

A drawback to the control system design presented thus far is that the vehicle parameters are not precisely known and they vary due to winds. Also, the gain constants cannot be set exactly. Due to these factors, the pitch response cannot be followed exactly. The second order system was therefore run with an integral gain term added to the deflection angle equation. By design, the system with integral gain always follows the pitch program at low frequencies regardless of vehicle parameter and gain constant variation during flight. The control equation for this case is:

$$\delta = \left(1 + \frac{K_I}{s}\right) K_p(\theta_p - \Delta\theta) - K_R \Delta\dot{\theta} - K_\alpha\alpha$$

The value of the integral gain constant (K_I) was chosen by specifying the third pole of the system (β) and equating coefficients. Since larger β values result in a faster pitch response and also a larger deflection angle requirement, β is chosen as small as possible to yield a satisfactory pitch response. The value of β was selected to be

0.3 radian per second. With this value, it is shown that the deflection requirement does not increase appreciably above the requirement obtained without integral gain.

RESULTS AND DISCUSSION

The vehicle, trajectory, and aerodynamic parameters used are those of a large solid launch vehicle consisting of a 260-inch solid first stage, SIVB second stage, and extended Voyager payload. This vehicle is discussed in detail in reference 3. The vehicle parameters (table I) were chosen to correspond to maximum dynamic pressure flight conditions, since maximum deflection angle requirements occur at about this time. However, the reduction in deflection requirements is also applicable for other flight conditions. The control system undamped natural frequency and damping ratio were specified to be 1 radian per second and 0.707, respectively. These values were taken from reference 3.

TABLE I. - 260-INCH SOLID-VOYAGER VEHICLE PARAMETERS

Parameter	Value
Distance from gimbal point to center of gravity, a, m	23.6
Distance from center of gravity to center of pressure, b, m	17.4
Axial drag, F_A, N	1.08×10^6
Normal force per angle of attack, F_n, N/rad	7.92×10^6
Moment of inertia, I, kg-m^2	2.17×10^8
Mass, m, kg	1.11×10^6
Thrust, T, N	24.7×10^6
Velocity, v, m/sec	583.4
Nominal flight-path angle, γ_N, deg	45.0

The extended Voyager vehicle was chosen as an example since it has the greatest deflection angle requirement of solid fuel vehicles under study (ref. 1). The selection of this launch vehicle does not limit this analysis to only one vehicle. Appendix C presents a generalization of the vehicle equations developed and demonstrates that the analysis is applicable to other solid propellant launch vehicles.

The linearized equations of motion and control equation were programmed and run on a digital computer. Wind duration (τ) ranged from 3 to 20 seconds. From reference 2, the wind duration which has the largest deflection angle requirement for the launch vehicle under study is 4 seconds. Therefore, this τ value was investigated extensively. The wind duration range was extended to 20 seconds because typical durations are about 10 to 15 seconds. Also, this expanded range allows for application to other vehicles whose

wind duration area of interest may be considerably different. Several values of K_α were investigated. The program satisfactorily solved for the pitch and disturbance responses for both the second (with and without an integral gain term added) and third order approximations.

Figure 3 shows the values of the gain constants required to satisfy the desired transfer function, as a function of K_α, for the second and third order equations. K_γ does not exist for the second order case; the other constants are identical for the second and third order equations.

Figures 4(a) and (b) present the maximum deflection ratio, δ_R, (δ_R is defined as the deflection angle divided by the maximum wind angle) against wind duration for symmetrical triangular wind disturbances with total duration from 3 to 20 seconds. The angle of

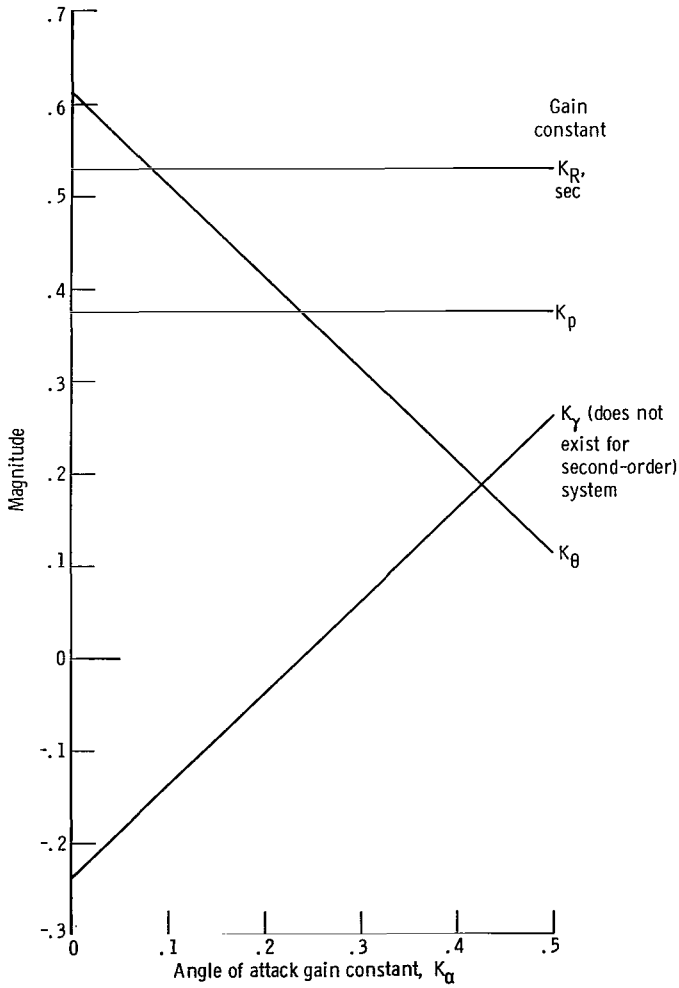

Figure 3. - Variation of feedback gain constants as functions of angle-of-attack gain constant.

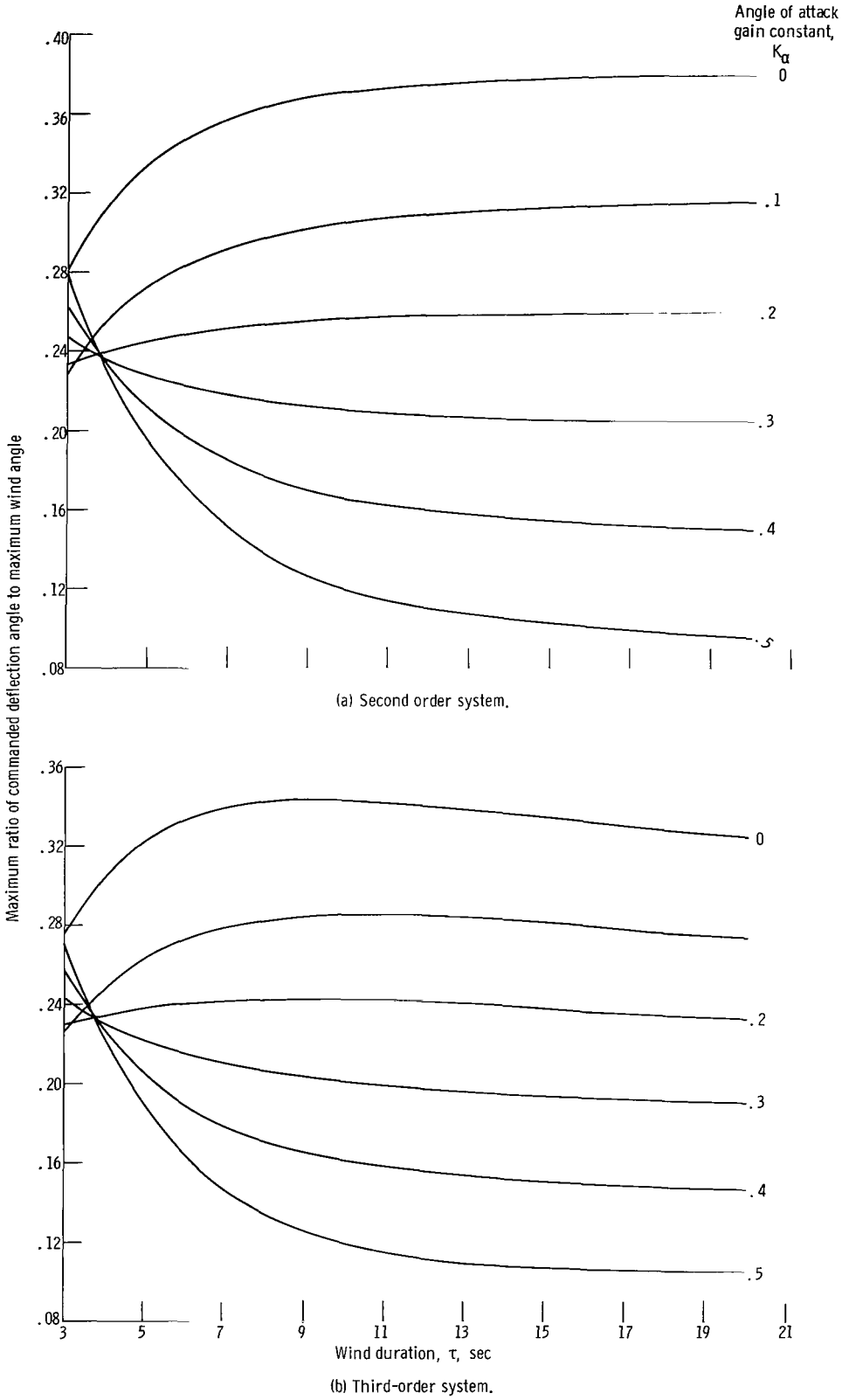

Figure 4. - Maximum value of ratio of deflection angle to maximum wind angle as function of symmetrical wind duration for various angle of attack gain constants.

attack gain constant (K_α) is varied between 0 and 0.5. The results in figure 4(a) are for the second order equations, while figure 4(b) presents the results for the third order equations. The results are similar with the third order system requiring a smaller $\delta_{R,max}$ for small K_α. This is due to drift, which reduces the angle of attack and, hence, the deflection angle required to control the vehicle. For both the second and third order systems, conventional autopilots ($K_\alpha = 0$) require significantly larger deflection angles than those required for load relief autopilots for wind durations greater than about 3 seconds. The largest reduction in deflection requirements is obtained by using the largest possible value of K_α. However, a limiting factor for choosing the magnitude of K_α is the possible high frequency noise in the angle of attack sensor. Therefore, $K_\alpha = 0.5$ was chosen to be a particular interest since this is the smallest value which is large enough to result in a substantial reduction in deflection angle requirements.

For short wind duration, the $K_\alpha = 0.5$ autopilot commands larger deflection angles than the conventional autopilot. However, it will be demonstrated in later figures that the commanded deflection angle for short wind durations is unnecessarily large (for $K_\alpha = 0.5$) and that the vehicle remains stable when a maximum deflection angle ($\delta_{R,max}$) smaller than the commanded value is used. It will also be shown that the deflection requirements can be reduced for $K_\alpha = 0$ and large wind durations, but this reduction is much smaller than that which is obtained by using a $K_\alpha = 0.5$ autopilot.

Figure 5 illustrates the wind angle, angle of attack, and deflection profiles for a typical wind with a peak at 3 seconds and a total duration of 12 seconds, for $K_\alpha = 0.5$.

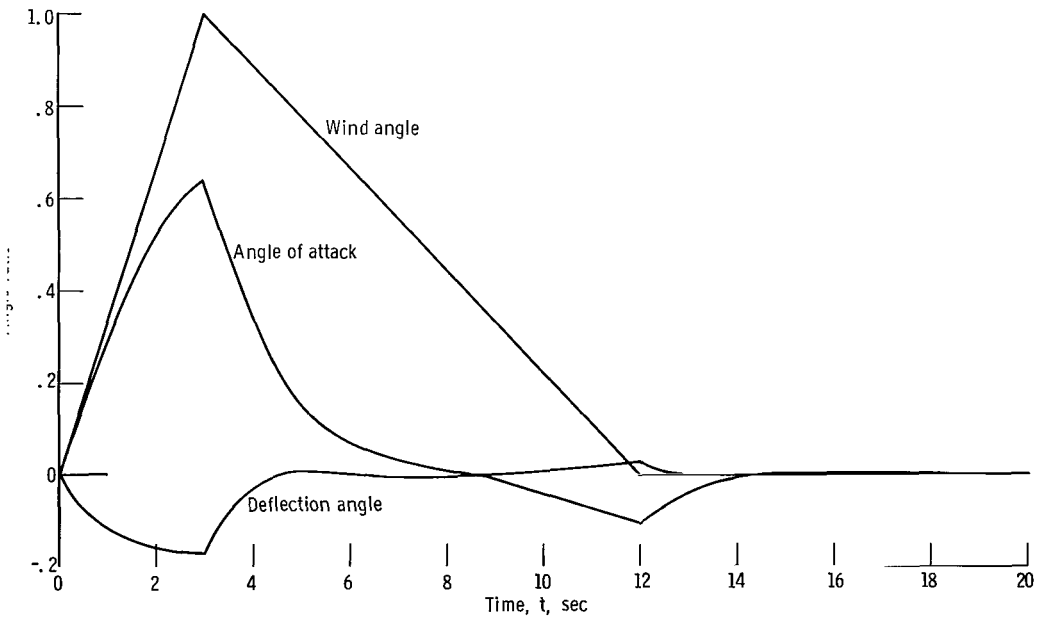

Figure 5. - Wind angle, angle of attack, and deflection angle as functions of time for a triangular wind disturbance.

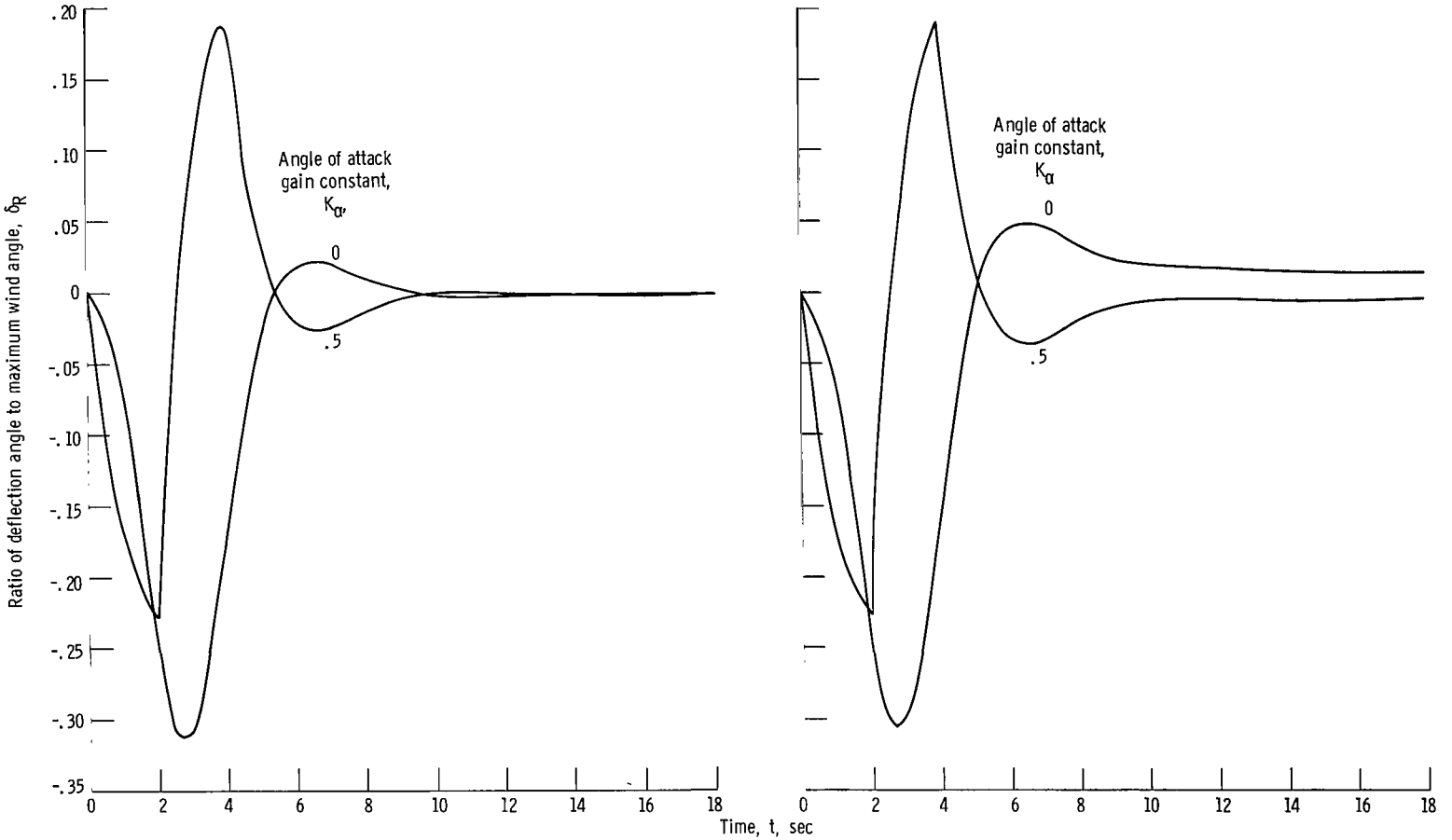

(a) Second-order system.

(b) Third-order system.

Figure 6. - Deflection response for a symmetrical triangular wind disturbance of 4 seconds.

The load relief action of the autopilot is evidenced by the fact that the vehicle angle of attack is smaller than the wind angle. For a conventional autopilot, the angle of attack and wind angle would be identical for the second order approximation.

Figures 6(a) and (b) present the δ_R response transients for a symmetrical triangular wind of 4 seconds duration with K_α values of 0 and 0.5. Here, figure 6(a) is for the second order analysis and 6(b) for the third order one. It is shown that the higher value of K_α commands a larger δ_R for about the first two seconds, which results in a lower maximum deflection requirement ($\delta_R = 0.23$ for $K_\alpha = 0.5$ and $\delta_R = 0.31$ for $K = 0$). Also, it is interesting to note that the integral of the absolute value of δ_R is about 20 percent less for $K_\alpha = 0.5$ than $K_\alpha = 0$. This is of particular importance when liquid injection is used for obtaining thrust vector control since 20 percent less fuel is required for $K_\alpha = 0.5$. Also, it can be observed from figure 6 that engine gimbal actuator requirements have not been significantly increased by the use of the load relief autopilot.

Figure 7 presents δ_R for a symmetrical triangular wind of 4 seconds duration and $K_\alpha = 0$. Two curves are illustrated; one with no limit on δ_R and the other with a limit of $\delta_{R,\max} = 0.240$. This graph demonstrates that a stable system can be maintained when the deflection angle is limited for the $K_\alpha = 0$ case. The maximum deflection requirement is 0.31, but δ_R can be limited to 0.240 and the system remains stable. This is accomplished by using $\delta_R = \delta_{R,\max}$ from about 2 seconds to 6.8 seconds. Prior to 2 seconds and after 6.8 seconds, δ_R is less than $\delta_{R,\max}$. Trim conditions are essentially

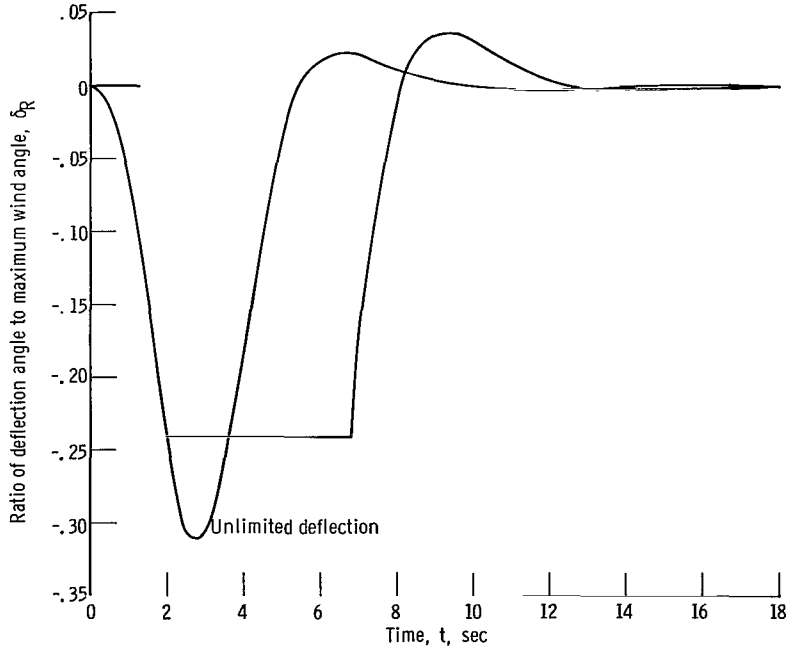

Figure 7. - Deflection response for a symmetrical triangular wind of 4 seconds, with and without deflection-angle limit. Angle of attack gain constant, K_α, 0.

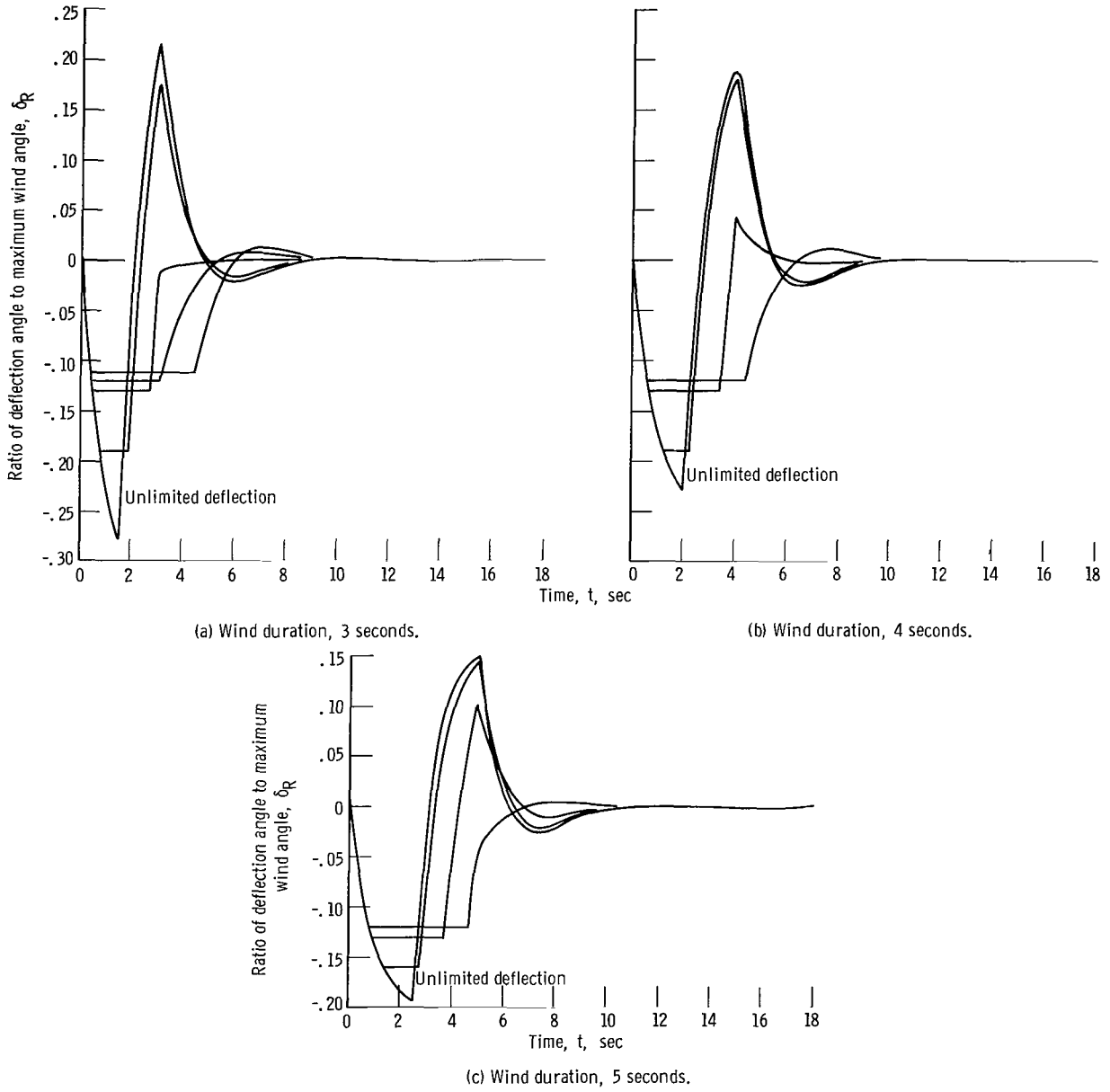

(a) Wind duration, 3 seconds.

(b) Wind duration, 4 seconds.

(c) Wind duration, 5 seconds.

Figure 8. - Deflection response with various deflection-angle limits. Angle of attack gain constant, K_α, 0.5; symmetrical triangular wind disturbance.

reestablished at about 13 seconds or about 9 seconds after the wind has subsided. Therefore, for $K_\alpha = 0$, the requirement cannot be reduced below about 0.24.

Figures 8(a), (b), and (c) present the deflection ratio response for symmetrical triangular winds of 3, 4, and 5 seconds duration, respectively, with $K_\alpha = 0.5$. The deflection ratio responses are shown for various values of $\delta_{R,max}$. The $\delta_{R,max}$ values presented on these figures are the smallest values investigated which result in a stable system, plus three additional values. It can be seen from the figure that for $\tau = 3$ seconds, $\delta_{R,max}$ can be reduced to 0.115; for $\tau = 4$ seconds, $\delta_{R,max} = 0.12$; for $\tau = 5$ seconds, $\delta_{R,max} = 0.12$, and the vehicle remains stable.

From figures 8(a), (b), and (c), $\delta_{R,max} = 0.120$ is the minimum value which results in a stable system for a wind duration range of 3 to 5 seconds. This value of $\delta_{R,max}$ was investigated in figure 9 for 6, 8, and 10 seconds duration winds with $K_\alpha = 0.5$. Longer wind durations were not examined since they never have a commanded deflection requirement greater than 0.120 (fig. 4(a)). Figure 9 demonstrates that a limit as small as 0.120 can be used and still result in stable system.

Figure 10 presents the ratio of attitude deviation to maximum wind angle (θ_R) response curves for a triangular wind of 4 seconds duration with K_α values of 0 and 0.5. The θ_R response curves for 3, 4, and 5 seconds duration triangular winds are plotted

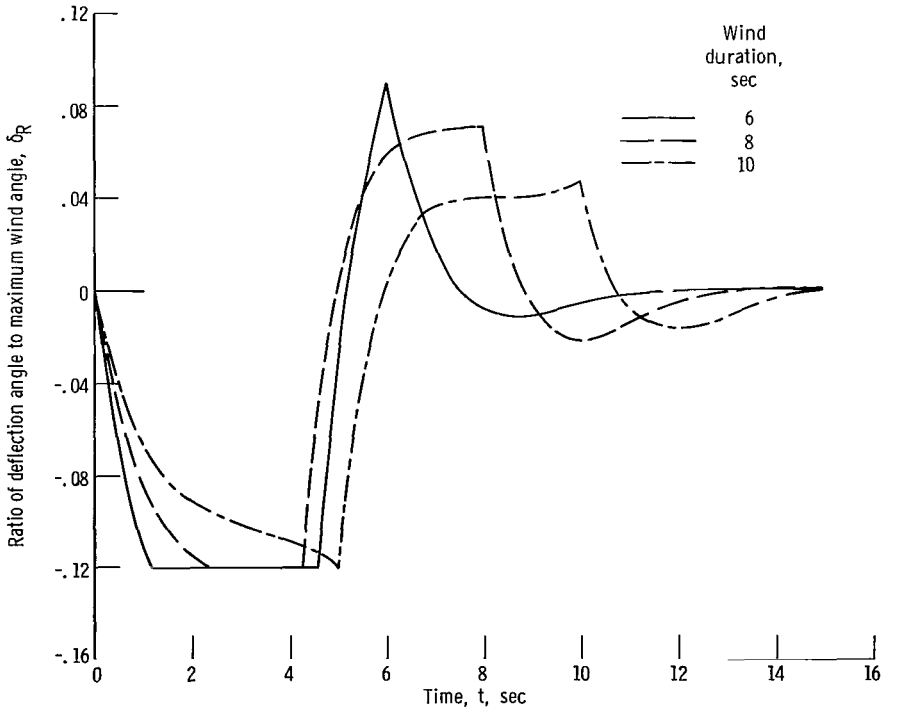

Figure 9. - Deflection response for symmetrical triangular winds of 6, 8, and 10 seconds. Deflection ratio limit, 0.12; angle of attack gain constant, K_α, 0.5.

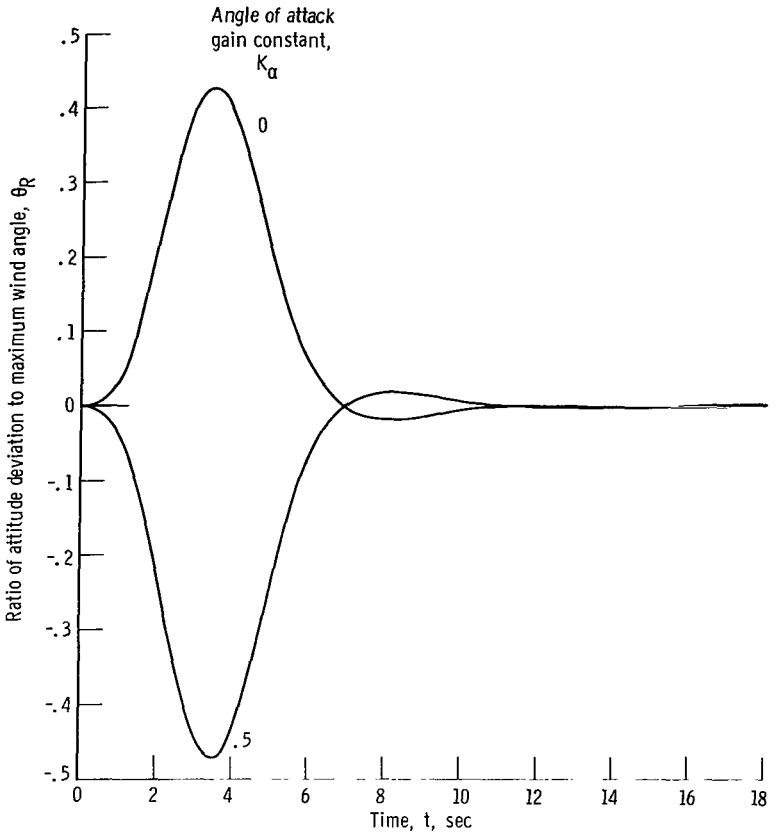

Figure 10. - Attitude response for symmetrical triangular wind disturbance of 4 seconds.

in figures 11(a), (b), and (c), respectively. Here, $K_\alpha = 0.5$ and curves are presented where the maximum deflection ratio is limited to the minimum values found for a stable system in the corresponding deflection angle analysis (fig. 8). These curves demonstrate that the attitude deviations are acceptable for the minimum $\delta_{R,max}$ cases.

It has been shown that a deflection ratio limit of 0.120 can be used and still result in a stable system for symmetrical triangular winds. This is significant since the requirement for a conventional autopilot designed to trim the vehicle ($K_\alpha = 0$), is 0.240. This results in a reduction in deflection requirements of about 50 percent for the autopilot analyzed. According to reference 2, the deflection requirement can be reduced to 38 percent of the trim value with an ideal autopilot design. With a more reasonable design, however, the requirement was 56 percent of the trim value. Therefore, the closed loop autopilot analyzed herein has achieved the reduction in deflection requirements indicated by reference 2.

Since actual flight winds are not always symmetric in shape, deflection requirements were also studied for unsymmetrical triangular winds with the $K_\alpha = 0.5$ autopilot. A range of time of peak wind (τ_1) of 3 to 10 seconds was investigated, with total wind dura-

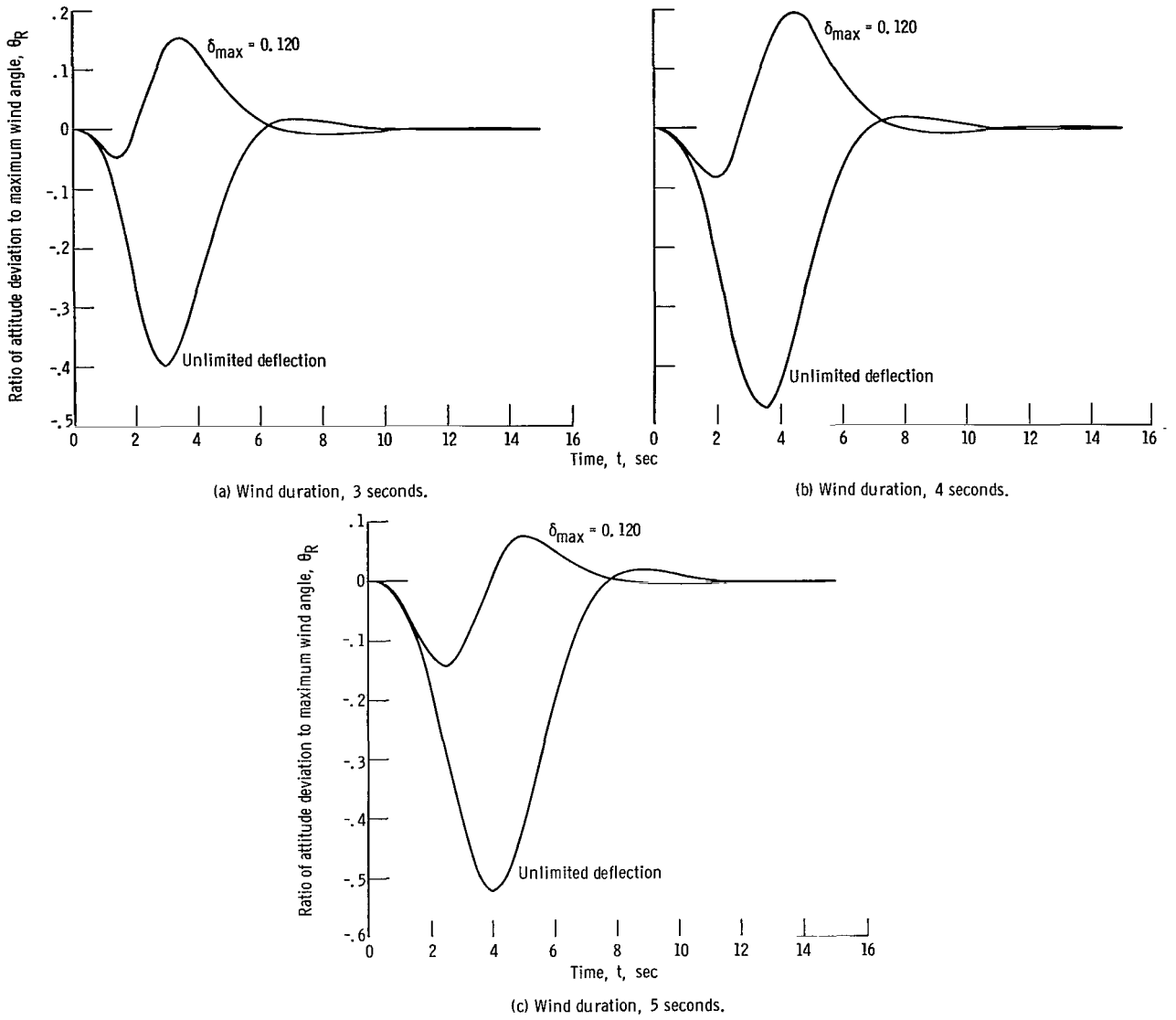

Figure 11. - Attitude response with and without deflection-angle limit. Angle of attack gain constant, K_α, 0.5; symmetrical triangular winds.

tion ranging from $(\tau_1 + 2)$ to $(\tau_1 + 10)$ seconds. Since the peak deflection requirement for $K_\alpha = 0.5$ always occurs at the peak of the wind (e.g., fig. 5), the maximum deflection ratio for an unsymmetrical wind with time of peak wind τ_1 is the same as for a symmetrical wind of total duration $\tau = 2\tau_1$. Therefore, the maximum deflection ratio against wind duration results can be obtained from figures 4(a) and (b).

The deflection ratio limit of 0.120 was then tested for each unsymmetrical wind which has a commanded deflection ratio greater than this value. It was found that the vehicle is stable with $\delta_{R,max} = 0.120$ for all winds with τ_1 not less than 4 seconds. For a τ_1 of three seconds, a $\delta_{R,max}$ of 0.130 was required for stability. Therefore, the pre-

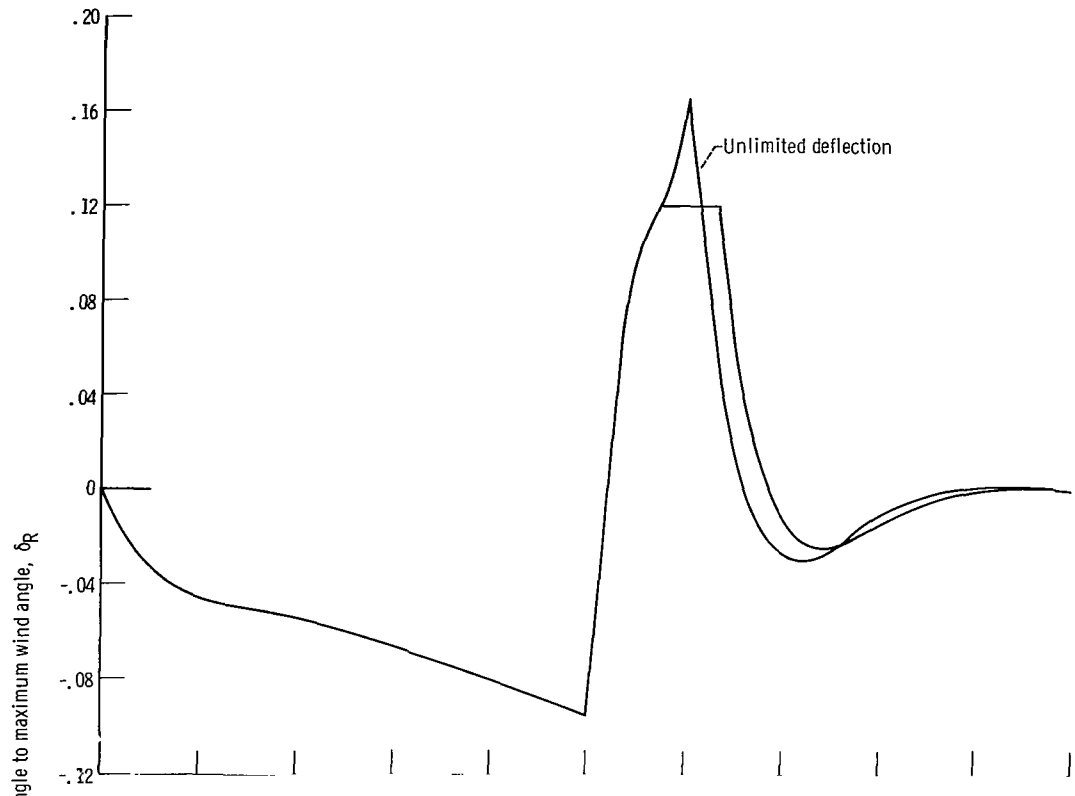

(a) Time of peak wind, 10 seconds.

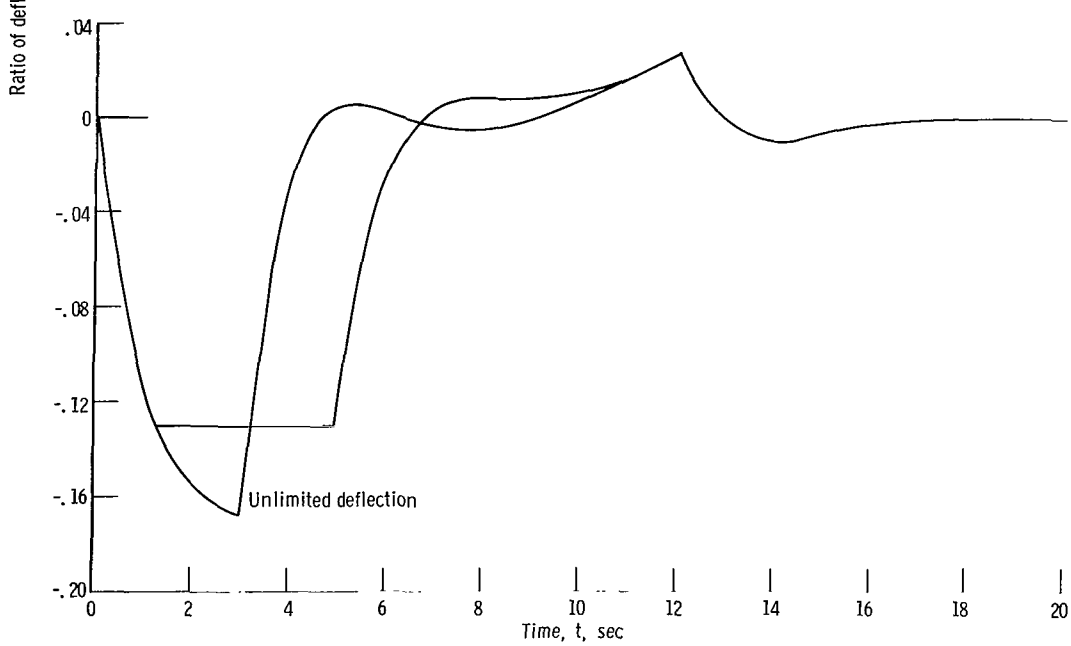

(b) Time of peak wind, 3 seconds.

Figure 12. - Deflection response for unsymmetrical triangular winds, with and without deflection-angle limit. Angle of attack gain constant, K_α, 0.5; wind duration, 12 seconds.

viously obtained reduction in deflection requirements has been slightly degraded for this case. However, a τ_1 of three seconds corresponds to an extremely rapid (and unlikely) wind buildup rate. For example, for a peak wind velocity of 60 meters per second, a τ_1 of three seconds corresponds to a wind shear of 0.049 meters per second per meter. That is, the wind velocity increases from 0 to 60 meters per second in an altitude interval of 1236 meters.

Figures 12(a) and (b) present deflection ratio responses for two typical unsymmetrical winds, by using second order equations and $K_\alpha = 0.5$. The figures show the unlimited δ_R profiles, as well as the stable limited cases.

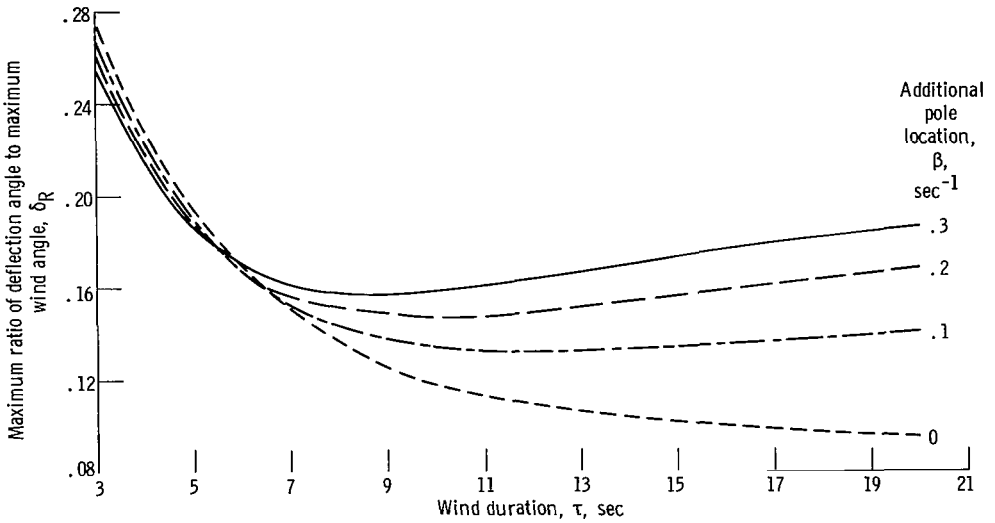

Figure 13. - Maximum value of ratio of deflection angle to maximum wind angle as function of symmetrical wind duration. Angle of attack gain constant, K_α, 0.5; second-order system with integral gain.

Figures 13 to 16 illustrate results for the integral gain system (the second order system with the integral gain added). In figure 13, maximum deflection angle ratio against wind duration is plotted for symmetrical triangular winds with $K_\alpha = 0.5$ and $\beta = 0$, 0.1, 0.2, and 0.3 radians per second. The wind duration range is from 3 to 20 seconds. Observe that the addition of the integral gain results in an increased deflection requirement for long wind durations. Also, the higher values of β result in larger deflection angle requirements for wind durations greater than about 6 seconds. The increased δ_R is a result of the integral gain forcing the attitude error to zero. This increases the angle of attack and, therefore, results in a larger δ_R.

Figure 14 compares the δ_R response for the second order analysis with that of the third order one which results from the addition of integral gain. It is seen that these

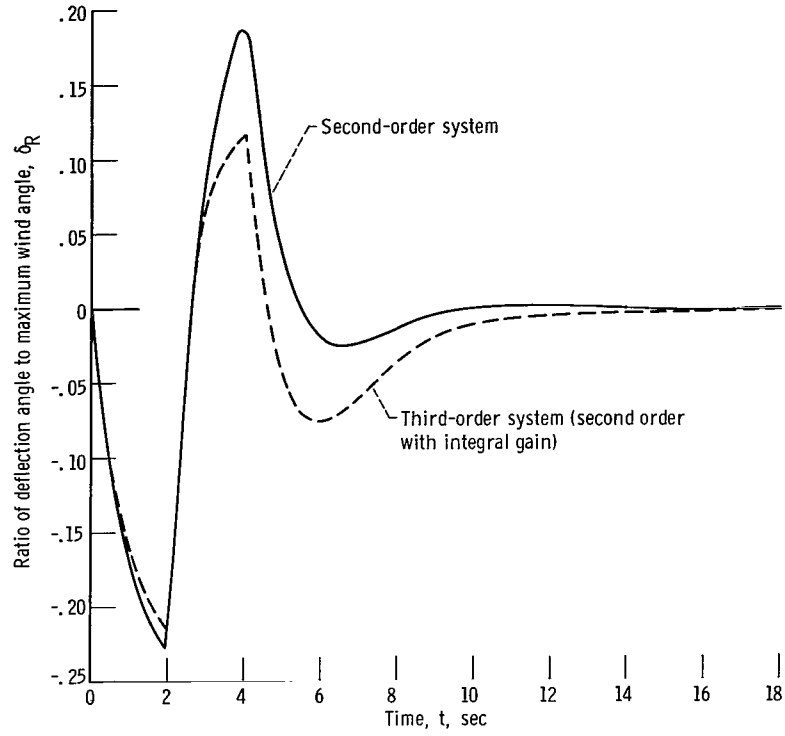

Figure 14. - Comparison of deflection response for symmetrical triangular wind disturbance of 4 seconds. Angle of attack gain constant, K_α, 0.5.

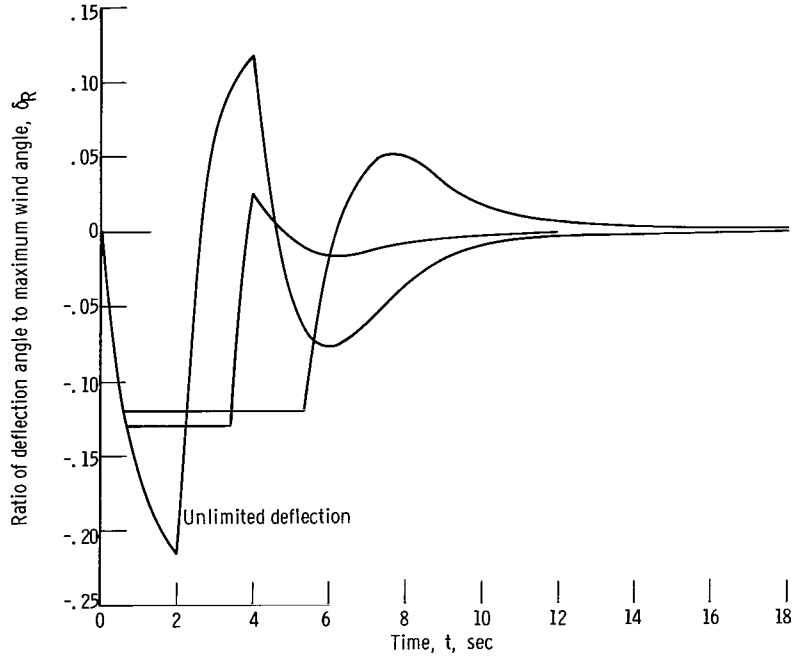

Figure 15. - Deflection response with various deflection angle limits for symmetrical triangular wind of 4 seconds. Angle of attack gain constant, K_α, 0.05; second-order system with integral gain.

transients are reasonably similar with a slightly larger deflection requirement for the second order system.

Figure 15 presents the deflection ratio response for the system with integral gain. With a wind duration of 4 seconds and $K_\alpha = 0.5$, the system was investigated with a limited δ_R in order to make a comparison with the corresponding second order analysis. The same deflection limits are used as for the second order case; and it is seen that the system with integral gain is also stable for these values.

Since longer wind durations result in an increased deflection angle requirement, a wind duration range of 10 to 22 seconds is investigated in figure 16. A stability map for the integral gain system is plotted in this figure. Analyzing the results, it is seen that for wind durations of up to 20 seconds, a minimum δ_{max} of 0.170 is required as compared to 0.120 for the second order system. However, for long duration winds, the flight parameters are not constant as is assumed by this analysis. Since the analysis is made at the maximum dynamic pressure point, δ_{max} required other than at this point will be lower for the same wind. Therefore, the 0.170 value is unrealistically high. In addition, β can be reduced in the high wind region so as to decrease the angle of attack and therefore the deflection requirement.

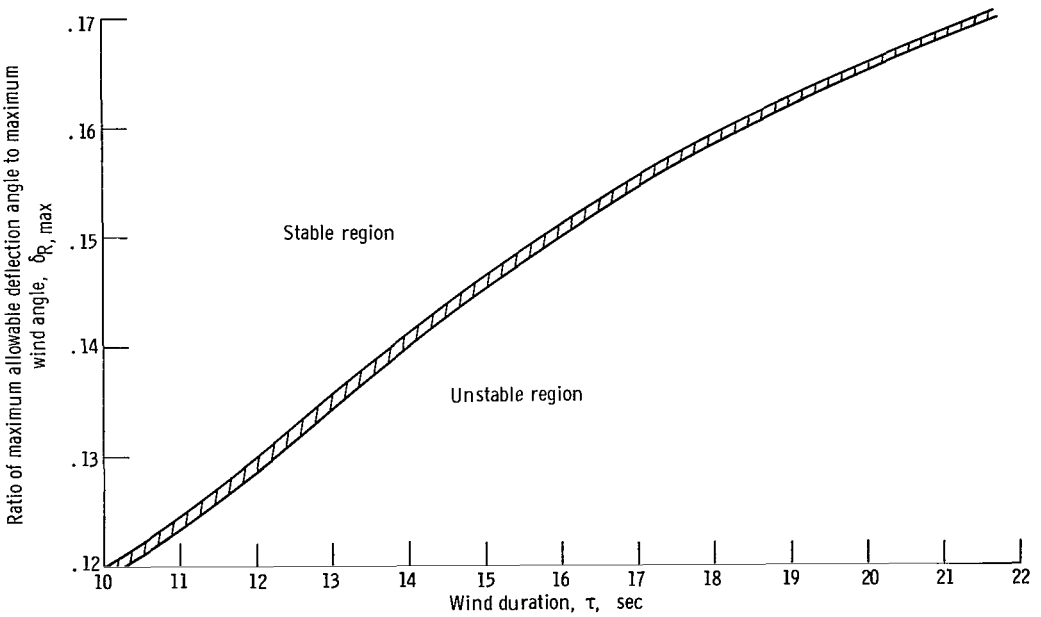

Figure 16. - Deflection ratio required for stability. Symmetrical triangular winds; second-order system with integral gain; additional pole location, β, 0.3 second^{-1}; angle of attack gain constant, K_α, 0.5.

CONCLUDING REMARKS

An autopilot has been analyzed which reduces the deflection angle required for flight

through design winds. This reduction is 50 percent of the requirement necessary to fly a vehicle under trimmed conditions. The autopilot analyzed requires the feedback of angle of attack and flight path angle in addition to attitude error and attitude rate.

The vehicle parameters simulated are those of a large solid launch vehicle consisting of a 260-inch solid motor first stage, SIVB second stage, and an extended Voyager payload. However, the equations developed may be applied to any launch vehicle. In addition, it was demonstrated that the results also apply to other solid propellant launch vehicles.

Third order equations were used to simulate the system. Also, integral gain was investigated. It was shown that the results of both of the above representations were the same as approximated by a system of second order equations.

The 50 percent reduction in deflection requirements obtained applies to the requirement due to wind disturbances only, and not to requirements due to thrust misalinement, center of gravity offset, other vehicle dispersions, or pitchover. However, these requirements are usually much smaller than the wind requirement. For example, for the Voyager vehicle, the wind requirement is 2.3°, the misalinement requirement is 0.25°, and the requirement due to the pitch program is 0.6° (ref. 1).

A rigid body configuration, as well as perfect angle of attack and flight path angle sensors, has been assumed. Further analysis is required to determine the effect of an imperfect sensor, actuator dynamics, and vehicle bending and sloshing effects.

Lewis Research Center,
National Aeronautics and Space Administration,
Cleveland, Ohio, June 17, 1968,
125-17-05-01-22.

APPENDIX A

SYMBOLS

a	distance from gimbal point to center of gravity, m
b	distance from center of gravity to center of pressure, m
CG	center of gravity
CP	center of pressure
c	additional pole in third order analysis, sec^{-1}
F_A	axial drag, N
F_n	normal force per angle of attack, N/rad
GP	gimbal point
G(s)	gain function
g	gravitational acceleration, m/sec^2
I	moment of inertia, $kg\text{-}m^2$
K_I	integral gain constant
K_p	pitch gain constant
K_R	attitude rate gain constant, sec
K_α	angle of attack gain constant
K_γ	flight path angle gain constant
K_θ	attitude gain constant
K_1, K_2	generalized parameters (appendix C)
m	mass, kg
s	Laplace operator, sec^{-1}
T	thrust, N
t	time, sec
v	velocity, m/sec
y	wind angle, rad
α	vehicle angle of attack, rad
β	pole which results from the use of integral gain, sec^{-1}
γ	flight path angle, rad
$\Delta( )$	linearized variable
δ	thrust vector deflection angle
δ_{trim}	ratio of maximum deflection angle to maximum wind angle for trimmed flight
ζ	damping ratio
θ	vehicle attitude, rad
θ_p	commanded vehicle pitch attitude, rad
λ	dummy variable (appendix C), sec^{-1}
λ_1, λ_2	generalization variables (appendix C), sec^{-1}
μ_c	vehicle control parameter, sec^{-2}
μ_α	vehicle aerodynamic parameter, sec^{-2}
τ	total wind duration, sec
τ_1	wind buildup time, sec
ω_n	undamped natural frequency, rad/sec

Subscripts:

max	maximum value

N	nominal
R	ratio of variable to maximum wind angle
rel	relative
w	wind

Superscripts:

$\dot{}$	time derivative
$\ddot{}$	second time derivative

APPENDIX B

EQUATIONS OF MOTION

Third Order Analysis

The vehicle equations of motion for a rigid body configuration in the pitch plane (see fig. 1) are:

$$I\ddot{\theta} = Ta \sin \delta + F_n b\alpha$$

$$\alpha = \theta - \gamma + y$$

$$mv\dot{\gamma} = T \sin (\theta - \gamma - \delta) - F_A \sin (\theta - \gamma) + F_n \alpha \cos (\theta - \gamma) - mg \cos \gamma$$

$$m\dot{v} = T \cos (\theta - \gamma - \delta) - F_A \cos (\theta - \gamma) - F_n \alpha \sin (\theta - \gamma) - mg \sin \gamma$$

$$\sin y = \frac{v_w}{v_N} \sin \gamma_N$$

Although these equations are written for the pitch plane, the analysis can be applied to the yaw plane by setting $g = 0$.

The nominal trajectory is assumed to be zero angle of attack and zero wind ($\alpha_N = 0$, $y = 0$). Therefore, $\theta_N = \gamma_N$. The nominal deflection angle (δ_N) is also assumed to be zero. Linearizing about the nominal trajectory at constant time, the above equations reduce to:

$$I\,\Delta\ddot{\theta} = Ta\delta + F_n b\alpha$$

or

$$\Delta\ddot{\theta} = \mu_c \delta + \mu_\alpha \alpha \tag{B1a}$$

$$\alpha = \Delta\theta - \Delta\gamma + y \tag{B1b}$$

$$\Delta\dot{\gamma} = \frac{1}{mv_N}\left[(T - F_A)\,\Delta\theta - (T - F_A - mg \sin \gamma_N)\,\Delta\gamma - T\delta + F_n\alpha\right] + \frac{g}{v_N^2} \cos \gamma_N \Delta v \tag{B1c}$$

$$\Delta\dot{v} = - g \cos \gamma_N \Delta\gamma \tag{B1d}$$

$$y = \frac{v_w}{v_N} \sin \gamma_N \tag{B1e}$$

where

$$\mu_c = \frac{Ta}{I}; \qquad \mu_\alpha = \frac{F_n b}{I}$$

These equations can be applied to the yaw plane by setting $g = 0$ and $\gamma_N = 90$ degrees.

From reference 2, $\Delta\gamma$ is small, which results in a small Δv. Also, the variation of v leads to a low frequency "phugoid" mode which contributes negligibly to the vehicle response. Therefore, Δv and $\Delta\dot{v}$ are assumed to be zero in the analysis that follows.

The autopilot control law utilizes the feedback of all state variables as well as angle of attack and flight path angle, as was discussed earlier. The deflection angle is therefore expressed as:

$$\delta = K_p\theta_p - K_\theta \Delta\theta - K_R \Delta\dot{\theta} - K_\alpha\alpha - K_\gamma \Delta\gamma \tag{B2}$$

Rewriting equations (B1a) and (B1c) by substituting for α, using Laplace notation and assuming all initial conditions to be zero:

$$(s^2 - \mu_\alpha) \Delta\theta + \mu_\alpha \Delta\gamma - \mu_c\delta = \mu_\alpha y \tag{B2a}$$

$$-\left(\frac{T + F_n - F_A}{mv_N}\right) \Delta\theta + \left(s + \frac{T + F_n - F_A - mg \sin \gamma_N}{mv_N}\right) \Delta\gamma + \frac{T}{mv_N} \delta = \frac{F_n}{mv_N} y \tag{B2b}$$

$$(K_R s + K_\theta + K_\alpha) \Delta\theta + (K_\gamma - K_\alpha) \Delta\gamma + \delta = K_p\theta_p - K_\alpha y \tag{B2c}$$

Writing equations (B2) in matrix form:

$$\begin{pmatrix} s^2 - \mu_\alpha & \mu_\alpha & -\mu_c \\ -\dfrac{T + F_n - F_A}{mv_N} & s + \dfrac{T + F_n - F_A - mg \sin \gamma_N}{mv_N} & \dfrac{T}{mv_N} \\ K_R s + K_\theta + K_\alpha & K_\gamma - K_\alpha & 1 \end{pmatrix} \begin{pmatrix} \Delta\theta \\ \Delta\gamma \\ \delta \end{pmatrix} = \begin{pmatrix} \mu_\alpha y \\ \dfrac{F_n}{mv_N} y \\ K_p\theta_p - K_\alpha y \end{pmatrix}$$

Taking the determinant of the characteristic matrix, the characteristic polynomial (denominator of the transfer functions) is:

$$s^3 + \left[\frac{T + F_n - F_A - mg \sin \gamma_N}{mv_N} + \mu_c K_R - \frac{T}{mv_N}(K_\gamma - K_\alpha)\right] s^2$$

$$+ \left[-\mu_\alpha + \frac{\mu_\alpha T}{mv_N} K_R + \mu_c(K_\theta + K_\alpha) + \mu_c \frac{T + F_n - F_A - mg \sin \gamma_N}{mv_N} K_R\right] s$$

$$+ \left[\frac{\mu_\alpha}{mv_N}\left(mg \sin \gamma_N + (K_\theta + K_\gamma)T\right) + \frac{\mu_c}{mv_N}\left((T + F_n - F_A)(K_\gamma + K_\theta) - mg \sin \gamma_N (K_\theta + K_\alpha)\right)\right]$$

Applying Cramer's rule and using the superposition principle to solve for the variables $\Delta\theta$ and δ:

$\frac{\Delta\theta}{\theta_p}$ numerator:

$$\mu_c K_p \left[s + \frac{\left(1 + \dfrac{\mu_\alpha}{\mu_c}\right) T + F_n - F_A - mg \sin \gamma_N}{mv_N}\right]$$

$\frac{\Delta\theta}{y}$ numerator:

$$(\mu_\alpha - \mu_c K_\alpha) s + \frac{\mu_\alpha}{mv_N}\left[(1 - K_\gamma)\, T - F_A - mg \sin \gamma_N\right]$$

$$-\frac{\mu_c}{mv_N}\left[K_\alpha(T - F_A - mg \sin \gamma_N) + F_n K_\gamma\right]$$

$\frac{\delta}{\theta_p}$ numerator:

$$K_p\left[s^3 + \frac{T + F_n - F_A - mg \sin \gamma_N}{mv_N} s^2 - \mu_\alpha s + \frac{\mu_\alpha g \sin \gamma_N}{v_N}\right]$$

$\frac{\delta}{y}$ numerator:

$$-K_\alpha s^3 - \left[\mu_\alpha K_R + \frac{K_\alpha(T - F_A - mg \sin \gamma_N) + F_n K_\gamma}{mv_N}\right]s^2$$

$$-\mu_\alpha\left[K_\theta + \frac{K_R}{mv_N}(T - F_A - mg \sin \gamma_N)\right]s$$

$$-\frac{\mu_\alpha}{mv_N}\left[(T - F_A - mg \sin \gamma_N)K_\theta + (T - F_A)K_\gamma\right]$$

Two of the poles of the desired characteristic polynomial are specified by the choice of the undamped natural frequency and damping ratio. The third pole is chosen to cancel the zero of $\Delta\theta/\theta_p$. This results in nearly identical second and third order transfer functions, as will be shown later. The desired characteristic polynomial is:

$$\left(s^2 + 2\zeta\omega_n s + \omega_n^2\right)(s + c) = s^3 + (2\zeta\omega_n + c)s^2 + \left(2\zeta\omega_n c + \omega_n^2\right)s + c\omega_n^2$$

where

$$c = \frac{1}{mv_N}\left[\left(1 + \frac{\mu_\alpha}{\mu_c}\right)T + F_n - F_A - mg \sin \gamma_N\right]$$

The feedback gain constants K_R, K_θ, and K_γ are chosen in terms of K_α to satisfy the desired characteristic polynomial. Also, the gain constant K_p is chosen so that the

control system follows the pitch program in the absence of disturbances. This procedure results in:

$$K_R = \frac{2\zeta\omega_n}{\mu_c}$$

$$K_\theta = \frac{\omega_n^2 + \mu_\alpha}{\mu_c} - K_\alpha$$

$$K_\gamma = K_\alpha - \frac{\mu_\alpha}{\mu_c}$$

$$K_p = \frac{\omega_n^2}{\mu_c}$$

With the above values of c and the feedback gain constants, the response equations can now be written:

$$\frac{\Delta\theta}{\theta_p} = \frac{\mu_c K_p \left[s + \frac{\left(1 + \frac{\mu_\alpha}{\mu_c}\right) T + F_n - F_A - mg \sin\gamma_N}{mv_N} \right]}{\left(s^2 + 2\zeta\omega_n s + \omega_n^2\right)(s + c)}$$

or

$$\frac{\Delta\theta}{\theta_p} = \frac{\mu_c K_p}{s^2 + 2\zeta\omega_n s + \omega_n^2}$$

$$\frac{\Delta\theta}{y} = \frac{(\mu_\alpha - \mu_c K_\alpha) \left[s + \frac{\left(1 + \frac{\mu_\alpha}{\mu_c}\right) T + F_n - F_A - mg \sin\gamma_N}{mv_N} \right]}{\left(s^2 + 2\zeta\omega_n s + \omega_n^2\right)(s + c)}$$

or

$$\frac{\Delta\theta}{y} = \frac{\mu_\alpha - \mu_c K_\alpha}{s^2 + 2\zeta\omega_n s + \omega_n^2}$$

$$\frac{\delta}{\theta_p} = \frac{K_p\left(s^3 + \frac{T + F_n - F_A - mg \sin\gamma_N}{mv_N} s^2 - \mu_\alpha s + \mu_\alpha \frac{g \sin\gamma_N}{v_N}\right)}{\left(s^2 + 2\zeta\omega_n s + \omega_n^2\right)(s + c)}$$

or

$$\frac{\delta}{\theta_p} \approx \frac{K_p\left(s^2 - \mu_\alpha\right)\left(s - \frac{g \sin\gamma_N}{v_N}\right)}{\left(s^2 + 2\zeta\omega_n s + \omega_n^2\right)(s + c)}$$

$$\frac{\delta}{y} = \frac{1}{\left(s^2 + 2\zeta\omega_n s + \omega_n^2\right)(s + c)} \cdot \left\{ -K_\alpha s^3 \right.$$

$$- \left[\frac{\mu_\alpha}{\mu_c} 2\zeta\omega_n + \frac{K_\alpha(T - F_A - mg \sin\gamma_N) - F_n\left(K_\alpha - \frac{\mu_\alpha}{\mu_c}\right)}{mv_N}\right] s^2$$

$$- \mu_\alpha \left[\frac{\omega_n^2 + \mu_\alpha}{\mu_c} - K_\alpha - \frac{1}{mv_N}(T - F_A\ mg \sin\gamma_N) \frac{2\zeta\omega_n}{\mu_c}\right] s$$

$$\left. - \frac{\mu_\alpha}{mv_N}\left[(T - F_A - mg \sin\gamma_N)\left(\frac{\omega_n^2 + \mu_\alpha}{\mu_c} - K_\alpha\right) + (T - F_A)\left(K_\alpha - \frac{\mu_\alpha}{\mu_c}\right)\right]\right\}$$

$$\frac{\delta}{y} \approx \frac{-1}{\left(s^2 + 2\zeta\omega_n s + \omega_n^2\right)(s + c)}\left[K_\alpha s^2 + \frac{\mu_\alpha}{\mu_c} 2\zeta\omega_n s + \frac{\mu_\alpha}{\mu_c}\left(\omega_n^2 + \mu_\alpha - \mu_c K_\alpha\right)\right] \cdot$$

$$\left\{ s + \frac{\frac{1}{mv_N}\left[\left(\frac{\mu_\alpha}{\mu_c} - K_\alpha\right)(-mg \sin \gamma_N) + \frac{\omega_n^2}{\mu_c}(T - F_A - mg \sin \gamma_N)\right]}{\frac{\omega_n^2 + \mu_\alpha}{\mu_c} - K_\alpha} \right\}$$

Second Order Analysis

The linearized equations of motion (eqs. (B1a), (B1b), and (B1c)) presented in the first section of this appendix may be approximated by assuming that the flight profile does not deviate from the nominal profile, due to the presence of winds; that is, $\Delta\gamma = 0$. This is a valid assumption for most large launch vehicles, as is shown in reference 2. The resulting linearized equations of motion are second order and are given by:

$$\Delta\ddot{\theta} = \mu_c \delta + \mu_\alpha \alpha$$

$$\alpha = \Delta\theta + y$$

$$\delta = K_p \theta_p - K_\theta \Delta\theta - K_R \Delta\dot{\theta} - K_\alpha \alpha$$

Writing these equations in matrix form and solving for the $\Delta\theta$ and δ responses as in the third order case results in:

$$\frac{\Delta\theta}{\theta_p} = \frac{\mu_c K_p}{s^2 + \mu_c K_R s + \mu_c(K_\theta + K_\alpha) - \mu_\alpha} = \frac{\omega_n^2}{s^2 + 2\zeta\omega_n s + \omega_n^2}$$

$$\frac{\Delta\theta}{y} = \frac{\mu_\alpha - \mu_c K_\alpha}{s^2 + 2\zeta\omega_n s + \omega_n^2}$$

$$\frac{\delta}{\theta_p} = \frac{\frac{\omega_n^2}{\mu_c}\left(s^2 - \mu_\alpha\right)}{s^2 + 2\zeta\omega_n s + \omega_n^2}$$

$$\frac{\delta}{y} = \frac{-\left[K_\alpha s^2 + \frac{\mu_\alpha}{\mu_c} 2\zeta\omega_n s + \frac{\mu_\alpha}{\mu_c}\left(\omega_n^2 + \mu_\alpha\right) - \mu_\alpha K_\alpha\right]}{s^2 + 2\zeta\omega_n s + \omega_n^2}$$

where K_R and K_θ are chosen to satisfy the desired natural frequency and damping ratio and K_p is chosen to satisfy the desired pitch response.

$$K_R = \frac{2\zeta\omega_n}{\mu_c}; \qquad K_\theta = \frac{\omega_n^2 + \mu_\alpha}{\mu_c} - K_\alpha; \qquad K_p = \frac{\omega_n^2}{\mu_c}$$

Comparison of Formulations

Comparing the results of the second and third order analyses, it is seen that the feedback gain constants, K_p, K_R, and K_θ are identical for the two formulations. An additional gain constant, K_γ, exists for the third order formulation (and also in the real case). By setting the additional pole of the third order system equal to the zero of the pitch response, $\Delta\theta/\theta_p$ and $\Delta\theta/y$ are also identical for the two systems. The small zero and small pole occurring in the third order system do not contribute measureably to the deflection angle response. The vehicle response to wind disturbances can therefore be accurately simulated by using second order equations.

Integral Gain Analysis

In order to more closely approximate an actual control system, an integral term is added to the control variable of the second order system. This use of an integral gain term in the autopilot guarantees that the vehicle will follow the desired pitch program even if the autopilot or vehicle parameters are not accurately known. With

$$\delta = K_p\theta_p - K_\theta\,\Delta\theta - K_R s\,\Delta\theta - K_\alpha\alpha$$

let

$$K_p = K_\theta = \left(1 + \frac{K_I}{s}\right)K_p$$

Then the deflection angle becomes

$$\delta = \left(1 + \frac{K_I}{s}\right)K_p(\theta_p - \Delta\theta) - K_R s\,\Delta\theta - K_\alpha(\Delta\theta + y)$$

$$s\delta = (s + K_I)K_p(\theta_p - \Delta\theta) - K_R s^2\,\Delta\theta - K_\alpha(\Delta\theta + y)s$$

where $\alpha = \Delta\theta + y$ was used. Also,

$$\Delta\ddot{\theta} = \mu_c\delta + \mu_\alpha\alpha$$

or

$$\left(s^2 - \mu_\alpha\right)\Delta\theta - \mu_c\delta = \mu_\alpha y$$

Rewriting the above equations and applying Cramer's rule to solve for the gain constants and transfer functions results in:

$$\left[(s + K_I)K_p + K_R s^2 + K_\alpha s\right]\Delta\theta + s\delta = (s + K_I)K_p\theta_p - K_\alpha sy$$

$$\left(s^2 - \mu_\alpha\right)\Delta\theta - \mu_c\delta = \mu_\alpha y$$

$$\frac{\Delta\theta}{\theta_p} = \frac{\mu_c(s + K_I)K_p}{s^3 + \mu_c K_R s^2 + \left[\mu_c(K_p + K_\alpha) - \mu_\alpha\right]s + \mu_c K_I K_p}$$

The denominator must be set equal to

$$\left(s^2 + 2\zeta\omega_n s + \omega_n^2\right)(s + \beta) = s^3 + (2\zeta\omega_n + \beta)s^2 + \left(2\zeta\omega_n\beta + \omega_n^2\right)s + \beta\omega_n^2$$

Therefore,

$$K_p = \frac{2\zeta\omega_n\beta + \omega_n^2 + \mu_\alpha - \mu_c K_\alpha}{\mu_c}$$

$$K_R = \frac{2\zeta\omega_n + \beta}{\mu_c}$$

$$K_I = \frac{\beta\omega_n^2}{\mu_c K_p}$$

Discretion must be used in the selection of β. Larger β values result in both a faster pitch response and a higher deflection angle requirement for flying through winds. Therefore, β is assigned the smallest value possible which yields a satisfactory pitch response. In this case, $\beta = 0.3$ radian per second was chosen. The deflection requirement does not increase appreciably with this value.

The vehicle attitude response to a wind disturbance becomes:

$$\frac{\Delta\theta}{y} = \frac{(\mu_\alpha - \mu_c K_\alpha)s}{\left(s^2 + 2\zeta\omega_n s + \omega_n^2\right)(s + \beta)}$$

and the deflection angle transfer functions are:

$$\frac{\delta}{\theta_p} = \frac{\frac{2\zeta\omega_n\beta + \omega_n^2 + \mu_\alpha - \mu_c K_\alpha}{\mu_c} s^3 + \frac{\beta\omega_n^2}{\mu_c} s^2 - \frac{\mu_\alpha}{\mu_c}\left(2\zeta\omega_n\beta + \omega_n^2 + \mu_\alpha - \mu_c K_\alpha\right)s - \frac{\mu_\alpha}{\mu_c}\beta\omega_n^2}{\left(s^2 + 2\zeta\omega_n s + \omega_n^2\right)(s + \beta)}$$

$$\frac{\delta}{y} = \frac{-\left[K_\alpha s^3 \frac{\mu_\alpha}{\mu_c}(2\zeta\omega_n + \beta)s^2 + \frac{\mu_\alpha}{\mu_c}\left(2\zeta\omega_n\beta + \omega_n^2 + \mu_\alpha - \mu_c K_\alpha\right)s + \frac{\mu_\alpha}{\mu_c}\beta\omega_n^2\right]}{\left(s^2 + 2\zeta\omega_n s + \omega_n^2\right)(s + \beta)}$$

APPENDIX C

GENERALIZATION OF AUTOPILOT ANALYSIS

By applying the second order approximation of appendix B, the deflection angle to wind response equation is a function of only two vehicle parameters, μ_α and μ_c, and the autopilot natural frequency, ω_n.

$$\frac{\delta}{y}(s) = \frac{-\left[K_\alpha s^2 + 2\zeta\omega_n \frac{\mu_\alpha}{\mu_c} s + \mu_\alpha \left(\frac{\omega_n^2}{\mu_c} + \frac{\mu_\alpha}{\mu_c} - K_\alpha\right)\right]}{s^2 + 2\zeta\omega_n s + \omega_n^2}$$

where it is assumed that the same damping ratio is desired for all vehicles.

Two constants, K_1 and K_2, will now be defined in terms of the three parameters mentioned above. Letting

$$\omega_n^2 = K_1 \mu_\alpha$$

$$K_\alpha = K_2 \frac{\mu_\alpha}{\mu_c}$$

K_1 and K_2 can be evaluated. For the 260-inch solid Voyager vehicle with $K_\alpha = 0.5$, $K_1 = 1.57$ and $K_2 = 2.1$. Substituting K_1 and K_2 into the $(\delta/y)(s)$ equation results in

$$\frac{\delta}{y}(s) = -\frac{K_2 \frac{\mu_\alpha}{\mu_c} s^2 + 2\zeta \sqrt{K_1}\sqrt{\mu_\alpha} \frac{\mu_\alpha}{\mu_c} s + \mu_\alpha \left(K_1 \frac{\mu_\alpha}{\mu_c} + \frac{\mu_\alpha}{\mu_c} - K_2 \frac{\mu_\alpha}{\mu_c}\right)}{s^2 + 2\zeta \sqrt{K_1}\sqrt{\mu_\alpha}\, s + K_1 \mu_\alpha}$$

$$= -\frac{\mu_\alpha}{\mu_c}\left[\frac{K_2 \left(\frac{s}{\sqrt{\mu_\alpha}}\right)^2 + 2\zeta \sqrt{K_1}\left(\frac{s}{\sqrt{\mu_\alpha}}\right) + (K_1 - K_2 + 1)}{\left(\frac{s}{\sqrt{\mu_\alpha}}\right)^2 + 2\zeta \sqrt{K_1}\left(\frac{s}{\sqrt{\mu_\alpha}}\right) + K_1}\right]$$

Defining $(\delta_{trim}/y) = -(\mu_\alpha/\mu_c)$

$$\frac{\delta}{\delta_{trim}}(s) = \left[\frac{K_2\left(\frac{s}{\sqrt{\mu_\alpha}}\right)^2 + 2\zeta\sqrt{K_1}\left(\frac{s}{\sqrt{\mu_\alpha}}\right) + (K_1 - K_2 + 1)}{\left(\frac{s}{\sqrt{\mu_\alpha}}\right)^2 + 2\zeta\sqrt{K_1}\left(\frac{s}{\sqrt{\mu_\alpha}}\right) + K_1}\right] \cdot y\left(\sqrt{\mu_\alpha}\,\frac{s}{\sqrt{\mu_\alpha}}\right)$$

For the 260-inch solid-Voyager vehicle, let $\sqrt{\mu_\alpha} = \lambda_1$. Then

$$\left(\frac{\delta}{\delta_{trim}}(s)\right)_{Voyager} = \left[\frac{K_2\left(\frac{s}{\lambda_1}\right)^2 + 2\zeta\sqrt{K_1}\left(\frac{s}{\lambda_1}\right) + (K_1 - K_2 + 1)}{\left(\frac{s}{\lambda_1}\right)^2 + 2\zeta\sqrt{K_1}\left(\frac{s}{\lambda_1}\right) + K_1}\right] \cdot y\left(\lambda_1\,\frac{s}{\lambda_1}\right)$$

$$= F\left(\frac{s}{\lambda_1}\right)$$

For a second vehicle, define $\sqrt{\mu_\alpha} = \lambda_2$ and assume a wind profile with the same shape but scaled in time so that the wind duration is $\lambda_1/\lambda_2\tau$. Then

$$\left(\frac{\delta}{\delta_{trim}}(s)\right)_{vehicle\ 2} = \left[\frac{K_2\left(\frac{s}{\lambda_2}\right)^2 + 2\zeta\sqrt{K_1}\left(\frac{s}{\lambda_2}\right) + (K_1 - K_2 + 1)}{\left(\frac{s}{\lambda_2}\right)^2 + 2\zeta\sqrt{K_1}\left(\frac{s}{\lambda_2}\right) + K_1}\right] \cdot \frac{\lambda_1}{\lambda_2}\, y\left(\lambda_1\,\frac{s}{\lambda_2}\right)$$

$$= \frac{\lambda_1}{\lambda_2} F\left(\frac{s}{\lambda_2}\right)$$

From the definition of a Laplace transform, if

$$\mathcal{L}\{f(t)\} = F(s)$$

then

$$\mathcal{L}\{f(\lambda t)\} = \frac{1}{\lambda} F\left(\frac{s}{\lambda}\right)$$

Therefore,

$$\left(\frac{\delta}{\delta_{trim}}(t)\right)_{Voyager} = \mathcal{L}^{-1}\left\{F\left(\frac{s}{\lambda_1}\right)\right\} = \lambda_1 f(\lambda_1 t)$$

$$\left(\frac{\delta}{\delta_{trim}}\right)_{vehicle\ 2} = \mathcal{L}^{-1}\left\{\frac{\lambda_1}{\lambda_2} F\left(\frac{s}{\lambda_2}\right)\right\} = \lambda_1 f(\lambda_2 t)$$

That is, when using a different vehicle (vehicle 2), the wind duration (τ) need only be transformed by multiplying by (λ_1/λ_2) and the appropriate deflection ratio can be read from the figures presented.

In order for this generalization to be valid, $K_1 = 1.57$ must result in an acceptable ω_n (so not to excite the vehicle bending modes). Table II illustrates the μ_α and μ_c values for two other typical solid propellant rocket vehicles, the 260-inch solid. Apollo and SSOPM vehicles (ref. 1), in addition to the 260-inch solid-Voyager vehicle. The 260-inch solid-Apollo and Voyager vehicles are identical except for different payloads. The SSOPM vehicle has solid first and second stages and is designed to deliver one million pounds (450 000 kg) to a low earth orbit. The natural frequency for each vehicle is calculated and is seen to be reasonable (not appreciably different from the value selected for the Voyager vehicle). Any other vehicle can also be tested by solving for the ω_n value by using the generalization parameters, K_1 and K_2, and the

TABLE II. - VEHICLE PARAMETERS FOR GENERALIZATION OF AUTOPILOT DESIGN

Parameter	Vehicle		
	Voyager	Apollo	SSOPM
Vehicle aerodynamic parameter, μ_α, sec^{-2}	0.636	0.436	0.171
Vehicle control parameter, μ_c, sec^{-2}	2.67	2.67	1.4
Ratio of aerodynamic parameter to control parameter, μ_α/μ_c	0.238	0.163	0.122
Undamped natural frequency, ω_n, rad/sec	1.0	0.83	0.52

vehicle parameters μ_α and μ_c. If the calculated ω_n is acceptable, the user merely needs to translate the abscissa of the figures. If the ω_n value is not acceptable, new K_1 and K_2 values can be solved for and new deflection angle to wind duration curves must be plotted. Based on the results presented in reference 2, it is expected that the same 50 percent saving in deflection requirements would still be obtained.

REFERENCES

1. Teren, Fred; Davidson, Kenneth I.; Borsody, Janos; and Daniele, Carl J.: Thrust-Vector Control Requirements for Large Launch Vehicles with Solid-Propellant First Stages. NASA TN D-4662, 1968.

2. Borsody, Janos; and Teren, Fred: Stability Analysis and Minimum Thrust Vector Control Requirements of Booster Vehicles During Atmospheric Flight. NASA TN D-4593, 1968.

3. Dawson, R. P.: Saturn IB Improvement Study (Solid First Stage), Phase II, Final Detailed Report. Rep. SM-51896, vol. 2, Douglas Aircraft Co., Inc. (NASA CR-77129), Mar. 30, 1966.

NATIONAL AERONAUTICS AND SPACE ADMINISTRATION
WASHINGTON, D. C. 20546

OFFICIAL BUSINESS

FIRST CLASS MAIL

POSTAGE AND FEES PAID
NATIONAL AERONAUTICS AND
SPACE ADMINISTRATION

POSTMASTER: If Undeliverable (Section 158 Postal Manual) Do Not Return

"The aeronautical and space activities of the United States shall be conducted so as to contribute . . . to the expansion of human knowledge of phenomena in the atmosphere and space. The Administration shall provide for the widest practicable and appropriate dissemination of information concerning its activities and the results thereof."

—NATIONAL AERONAUTICS AND SPACE ACT OF 1958

NASA SCIENTIFIC AND TECHNICAL PUBLICATIONS

TECHNICAL REPORTS: Scientific and technical information considered important, complete, and a lasting contribution to existing knowledge.

TECHNICAL NOTES: Information less broad in scope but nevertheless of importance as a contribution to existing knowledge.

TECHNICAL MEMORANDUMS: Information receiving limited distribution because of preliminary data, security classification, or other reasons.

CONTRACTOR REPORTS: Scientific and technical information generated under a NASA contract or grant and considered an important contribution to existing knowledge.

TECHNICAL TRANSLATIONS: Information published in a foreign language considered to merit NASA distribution in English.

SPECIAL PUBLICATIONS: Information derived from or of value to NASA activities. Publications include conference proceedings, monographs, data compilations, handbooks, sourcebooks, and special bibliographies.

TECHNOLOGY UTILIZATION PUBLICATIONS: Information on technology used by NASA that may be of particular interest in commercial and other non-aerospace applications. Publications include Tech Briefs, Technology Utilization Reports and Notes, and Technology Surveys.

Details on the availability of these publications may be obtained from:

SCIENTIFIC AND TECHNICAL INFORMATION DIVISION

NATIONAL AERONAUTICS AND SPACE ADMINISTRATION

Washington, D.C. 20546